Simultaneous removal of lead, copper, cadmium, nickel, and cobalt heavy metal ions from the quinary system by *Abies bornmulleriana* cones

Ensar Oguz

ABSTRACT

Abies bornmulleriana cone was used to investigate its biosorption efficiency and capacity of Pb^{2+}, Cu^{2+}, Cd^{2+}, Co^{2+}, and Ni^{2+} heavy metal ions in a quinary system. The mechanism of multi-metal removal was illustrated in terms of FTIR results. Electrophoretic mobilities of the biosorbents were determined to access the information about the competitive biosorption. BET surface area and pore volume of the biosorbents before and after the biosorption were defined to be (5.05 $m^2\ g^{-1}$ and 0.0018 $cm^3\ g^{-1}$) and (0.97 $m^2\ g^{-1}$ and 0.00032 $cm^3\ g^{-1}$), respectively. The average pore width of the biosorbent before and after the biosorption was calculated as 9.34 and 13.04 Å, respectively. The pseudo-first-order model and the pseudo-second-order model were applied to analyze the experimental data. Experimental data have been evaluated according to the Langmuir, Freundlich, Temkin, and Dubinin-Radushkevich isotherms. The maximum biosorption efficiency and capacity for Pb^{2+}, Cu^{2+}, Cd^{2+}, Ni^{2+}, and Co^{2+} ions were defined as (85.4, 56.4, 35.4, 21.7 and 18.9%) and (8.5, 5.6, 3.5, 2.2 and 1.9 mg g^{-1}), respectively. The selectivity of heavy metal ions resulted in the magnitude order of $Pb^{2+} > Cu^{2+} > Cd^{2+} > Ni^{2+} > Co^{2+}$.

Key words | *Abies bornmulleriana* cone, multi-metals, quinary system, simultaneous biosorption

Ensar Oguz
Environmental Engineering Department,
Atatürk University,
25240 Erzurum,
Turkey
E-mail: *eoguz@atauni.edu.tr*; *ensaroguz25@gmail.com*

HIGHLIGHTS

- BET surface area of biosorbent after the competitive biosorption decreased.
- Changes in FTIR spectra after the competitive biosorption points out the biosorption of ions.
- Capacity for Pb^{2+} in the quinary systems was bigger than these of other ions.
- The variations in the zeta potentials were evidence of the biosorption of ions.
- Biosorption capacities of ions followed the magnitude order of $Pb^{2+} > Cu^{2+} > Cd^{2+} > Ni^{2+} > CO^{2+}$.

doi: 10.2166/wst.2020.547

GRAPHICAL ABSTRACT

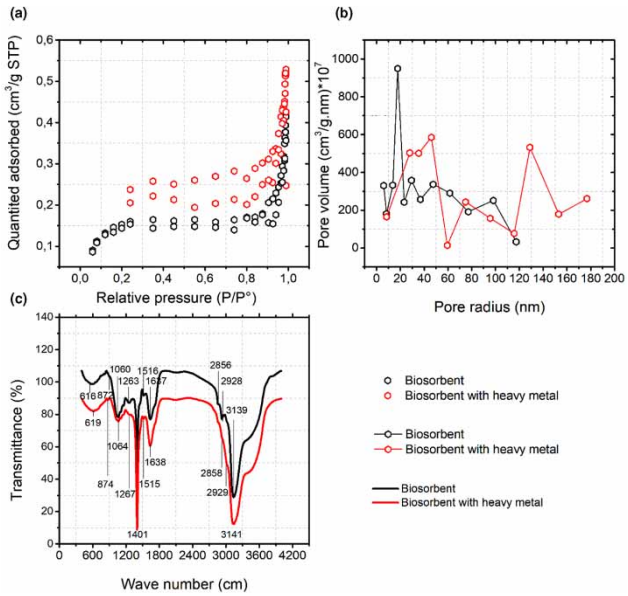

INTRODUCTION

Water is the primary matter for the presence of life, and for humanity, which improved on their civilizations by the side of water resources to promote the consumption of water (Vuorinen *et al.* 2007). Deterioration of water resources originating from heavy metal ions is a continual problem due to the inadequate discharging of industrial effluents such as printing processes, metallurgy, agricultural, and mining activities to the receiving environments (Munagapati *et al.* 2010).

Heavy metal ions can create many problems for the human body due to the distinctive physicochemical properties of each ion. Pb^{2+}, Cu^{2+}, Cd^{2+}, Co^{2+}, and Ni^{2+} metal ions originate from various industries. Some of them are micronutrients required for living organisms at trace amounts. But, excess intake of these heavy metal ions can give rise to health problems, including kidney and liver failure, gastrointestinal disturbance, birth defects, liver damage, hypertension, cancer, mental retardation, reduction in haemoglobin production, neurologic signs and depression (Kurniawan *et al.* 2006; Han *et al.* 2009; Laus & de Favere 2011). At present, the uptake of metal ions originating from wastewater is a primary matter for environmental organizations. Thus, it is required to keep under control the fraction of heavy metal ions in wastewaters before their discharge into the receiving environment.

The treatment of wastewater, including heavy metal ions, is a difficult task for environmental engineers, policymakers, and municipalities. Several technologies such as adsorption, catalysis, coagulation, electro/chemical reduction, advanced oxidation, biological treatment, and membrane separation processes are widely used in the removal of hazardous pollutants from wastewater (Ahsan *et al.* 2019, 2020b, 2020c; Islam *et al.* 2019). However, the adsorption process is one of the most effective, simple and low-cost techniques for the removal of organic and inorganic substances from wastewater (Hyder *et al.* 2014; Begum *et al.* 2016). Adsorbents obtained from polymeric materials, industrial solid wastes, and agricultural by-products have gained widespread attention in recent years for the removal of organic substance from wastewater (Begum *et al.* 2016; Peng *et al.* 2016; Islam *et al.* 2017; Liu *et al.* 2017).

The biosorption has been known to be a cost-effective alternative in the treatment of heavy metal ions (Volesky 2007). Usually, the biosorption technique can diminish operational costs by 36%, capital costs by 20% and total treatment cost by 28% compared with the standard methods (Loukidou *et al.* 2004). Therefore, the interest in the application of low-cost alternatives in recent years has considerably augmented. Biosorption is

the most investigated process for such kinds of waters containing heavy metal ions at trace dosages. It can be practiced on the treatment of wastewaters using inexpensive biosorbent materials such as wood waste, weeds and sawdust (Asadi *et al.* 2008; Pereira *et al.* 2010), sunflower biomass (Oguz & Ersoy 2010, 2014), yellow squash (Oguz & Utku 2019), sugarcane bagasse (Homagai *et al.* 2010), pulp and seeds (Liu *et al.* 2012; Torab-Mostaedi *et al.* 2013), wheat straw (Pehlivan *et al.* 2012), olive pomace and stone (Martin-Lara *et al.* 2012), etc.

In general, the evaluation of biosorption in the quinary system is more complicated than a single system due to the competitive interactions between heavy metal ions for the biosorbent sites. Multi-metal biosorption investigations are significant to evaluate the level of interference caused by co-ions available in the water and wastewater. Several studies have been conducted about the selectivity sequences of heavy metal ions in multi-component systems using different biosorbents; for example, biosorption of Pb^{2+}, Cu^{2+} and Ni^{2+} by native grapefruit (Bayo 2012), biosorption of Cu^{2+}, Pb^{2+}, Zn^{2+} and Cd^{2+} by cabbage waste (Hossain *et al.* 2014), biosorption of Pb^{2+}, Cd^{2+}, Cu^{2+}, Ni^{2+}, and Zn^{2+} by black gram husk (Saeed *et al.* 2005), and the biosorption of Cu^{2+} and Ni^{2+} by peat (Ho & McKay 1999a).

For the first time by this study, *Abies bornmulleriana* cones were utilised to define the biosorption efficiency and capacity of Pb^{2+}, Cu^{2+}, Cd^{2+}, Co^{2+}, and Ni^{2+} metal ions in the quinary system. The present investigation aimed to evaluate the ability of *Abies bornmulleriana* cone to treat multi-metal ions in the quinary system taking into account the competitive interactions of heavy metal ions. The influence of the various experimental parameters, including multi-metal ion concentration, pH, temperature, biosorbent quantity, particle size, and different salt types on the uptake of heavy metal ions was researched. Besides, the mechanism of multi-metal removal was illustrated in terms of FTIR results. Electrophoretic mobilities of *Abies bornmulleriana* cones were determined to gain information about the biosorption process. Pore volume and BET surface area of *Abies bornmulleriana* cones before and after the biosorption were defined to interpret the biosorption mechanism. Different kinetic studies were practiced to explain the experimental data. The selectivity of heavy metal ions in the competitive biosorption resulted in the magnitude order of $Pb^{2+} > Cu^{2+} > Cd^{2+} > Ni^{2+} > Co^{2+}$.

MATERIAL AND METHODS

Abies bornmulleriana cones

Abies bornmulleriana cones were obtained from Azdavay district of Kastamonu province in Turkey. The cones collected in August of 2016 were washed more than once with deionized water so that the ordinary impurities on the biosorbent surface could be removed. Afterwards, biosorbent particles were dried in the open air during 120 hours and were broken into small pieces, ground in a blender, and screened to classify by various particle sizes (0.25–0.250, 0.250–0.5, 0.5–1, and 1–2 mm).

Chemical solutions

All chemicals used in this investigation were of analytical grade from Sigma-Aldrich (USA) and were used as obtained. The stock solutions containing 200 mg L^{-1} of Pb^{2+}, Cu^{2+}, Cd^{2+}, Ni^{2+}, and Co^{2+} metal ions were prepared by dissolving lead, copper, cadmium, nickel and cobalt nitrate salt, Pb^{2+} [$(Pb(NO_3)_2]$, Cu^{2+} [$Cu(NO_3)_2.3H_2O$], Cd^{2+}[$Cd(NO_3)_2.4H_2O$], Ni^{2+}[$Ni(NO_3)_2.6H2O$], and Co^{2+} [$Co(NO3)_2.6H2O$]. Additionally, to evaluate the influence of Ca^{2+}, Na^{+} and K^{+} ions on Pb^{2+}, Cu^{2+}, Cd^{2+}, Ni^{2+} and Co^{2+} biosorption, 200 mg L^{-1} analytical grade stock solutions of Ca^{2+}[$(CaNO_3)$], Na^{+}[$(NaNO_3)$] and K^{+}[(KNO_3)] were prepared and diluted to the desired concentration of 0.01 M. Nitrate salt of the metal ions was utilised as the counter ion because it has a low tendency to produce metal complexes All the heavy metal ions exist in their free form. The Pb^{2+}, Cu^{2+}, Cd^{2+}, Ni^{2+}, and Co^{2+} solutions were prepared by diluting a stock solution of 200 mg L^{-1} with pure water to a required concentration range between 20 and 60 mg L^{-1}.

Biosorption studies in the batch system

Biosorption investigations for Pb^{2+}, Cu^{2+}, Cd^{2+}, Ni^{2+}, and Co^{2+} ions in the multi-system were conducted at the concentrations of 20, 30, 40, 50 and 60 mg L^{-1} to obtain the biosorption efficiencies and capacities. The pH of the solution was maintained by the addition of 0.1 M NH_3 and 0.1 M HNO_3. A known dosage of biosorbent (100 mg) was added to a series of 100 mL Erlenmeyer flasks containing 50 ML of heavy metal ions, which were located in the temperature-controlled shaker (Edmund Bühler Incubator

HoodTH15) during 1 h. After equilibrium, filter paper (Whatman No. 42) was utilised to separate the biosorbent particles from solutions, and the final concentration of the ions was defined by ICP-MS (Agilent 7800).

Surface structure and functional group analyses of *Abies bornmulleriana* cones

The cones surface area and pore volume were defined using a Quantachrome QS-17 model apparatus 35. Barrett-Joyner-Halenda (BJH) method was utilised to estimate the pore size distribution of the biosorbent particles. The total pore volume of the cones was defined at a relative pressure of 0.99. BET surface area and pore volume of cones before and after competitive biosorption were determined as ($5.05\ m^2\ g^{-1}$ and $0.0018\ cm^3\ g^{-1}$) and ($0.97\ m^2\ g^{-1}$ and $0.00032\ cm^3\ g^{-1}$), respectively. The average pore width of the biosorbent before and after competitive biosorption was calculated to be 9.34 and 13.04 Å, respectively.

A Perkin-Elmer 1720 spectrometer was utilised to take down Fourier transform infrared (FTIR) spectra of *Abies bornmulleriana* cones. In this investigation, the target of FTIR analysis is the observation of whether Pb^{2+}, Cu^{2+}, Cd^{2+}, Ni^{2+}, and Co^{2+} heavy metal ions adsorbed on *Abies bornmulleriana* cones alter the peaks of functional groups on the biosorbent.

The morphologic structure of the biosorbent surface was observed by using a scanning electron microscope with EDS spectroscopy (FE-SEM: Zeiss Sigma 300, USA).

Zeta potentials of *Abies bornmulleriana* cones were obtained to access advanced knowledge on the multi-component biosorption. The zeta potential measurements were carried out using a micro-electrophoresis cell (ZETA-METER 3:0-542, USA).

RESULTS AND DISCUSSION

Pore property, FTIR spectra, SEM images, and EDS analysis of *Abies bornmulleriana* cones

N_2 adsorption/desorption isotherms of *Abies bornmulleriana* cones before and after biosorption at 77 K are given in Figure 1(a). It is seen that the first part of the isotherms takes place at a lower relative pressure (P/P^o). The uptake of N_2, which increased quickly with the increase in the relative pressure, confirmed the availability of the meso and macropore structures. BJH technique was utilised to estimate the pore size distribution and volume of the biosorbents, and they are demonstrated in Figure 1(b). In Figure 1(b), the biosorbent before biosorption included macro and mesoporous volumes while the biosorbent after the biosorption included mainly macroporous volumes, as seen in Figure 1(b). The mesoporous volume of the biosorbent considerably decreased at the pore size of 20 nm. In contrast, the other mesoporous and macroporous volumes of the biosorbent generally increased after the biosorption, as presented in Figure 1(b). The BET surface area and pore volume of the biosorbent before and after the biosorption were defined to be ($5.05\ m^2\ g^{-1}$ and $0.0018\ cm^3\ g^{-1}$) and ($0.97\ m^2\ g^{-1}$ and $0.00032\ cm^3\ g^{-1}$), respectively. The average pore width of the biosorbent before and after the biosorption was calculated to be 9.34 and 13.04 Å, respectively.

FTIR spectroscopy was used to interpret the interchanges in the major functional groups of the biosorbent, and the interchanges are given in Figure 1(c). The FTIR spectra of *Abies bornmulleriana* cones describe many bands in the structure of the biosorbent. The changes in wavenumber and band intensity after the biosorption point out the functionalities of the biosorbent surface. Figure 1(c) indicates that some functional groups on the biosorbent are inclined to bind with the heavy metal ions. For instance, the peak at $3{,}139\ cm^{-1}$ was due to the vibration of the C-H stretching in 3-substituted pyrroles on the biosorbent. This peak shifted to $3{,}141\ cm^{-1}$ after the uptake of Pb^{2+}, Cu^{2+}, Cd^{2+}, Ni^{2+}, and Co^{2+} metal ions and shrank.

The peaks at 2,928 and $2{,}856\ cm^{-1}$ were related to OH stretching in the carboxylic acid groups and shifted to 2,929 and $2{,}858\ cm^{-1}$ after the biosorption. These changes in the biosorption bands illustrate that OH in the carboxylic acid was affected by binding with Pb^{2+}, Cu^{2+}, Cd^{2+}, Ni^{2+}, and Co^{2+} metal ions and shrank after the biosorption. The peaks appearing at 1,637 and $1{,}516\ cm^{-1}$ were associated with NH stretching vibration in the secondary amides (-CONH-) and shifted to 1,638 and $1{,}515\ cm^{-1}$ after the biosorption. The peaks at 1,262, 1,060 and $872\ cm^{-1}$ were related to aryl O stretching in the aromatic ethers, asymmetric C-O-C stretching in the aliphatic ethers, and symmetric C-O-C stretching in the vinyl ethers and shifted to 1,267, 1,064 and $874\ cm^{-1}$ after the biosorption. The peak at $616\ cm^{-1}$ was related to N-C = S deformation in the tertiary thioamides and shifted to $619\ cm^{-1}$ and shrank after the biosorption. It is estimated that there is an electrostatic and chemical attraction between the biosorbent sites and the metal ions. This interaction altered the charges on the biosorbent. Thus, the FTIR spectra of the functional groups on the biosorbent modified.

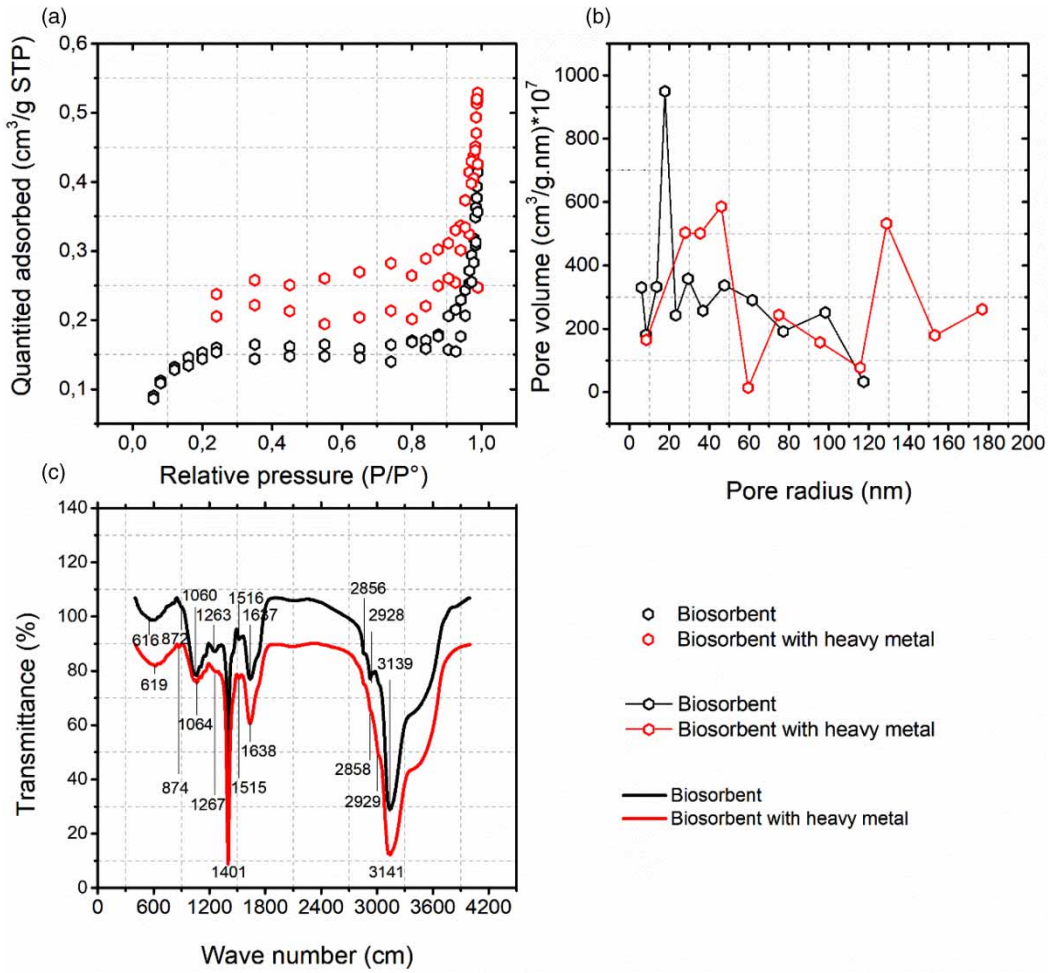

Figure 1 | (a) Nitrogen adsorption-desorption isotherms of *Abies bornmulleriana* cones at 77 K, (b) pore distributions of *Abies bornmulleriana* cones before and after the competitive biosorption in the competitive biosorption, (c) FTIR spectra of *Abies bornmulleriana* cones used in the quinary system before and after the competitive biosorption.

Figure 2(a) and 2(b) show the surface morphology of *Abies bornmulleriana* cones before and after the biosorption, respectively. The biosorbent not containing heavy metal ions (Pb^{2+}, Cu^{2+}, Cd^{2+}, Ni^{2+}, and Co^{2+}) appears to have an intact structure with groove rooms and an irregular surface. After the competitive biosorption, the pores were blocked and saturated due to the adsorption of the heavy metal ions (Pb^{2+}, Cu^{2+}, Cd^{2+}, Ni^{2+}, and Co^{2+}). Moreover, the cone's initial structure disappeared due to the metal ions' accumulation. Figure 2(c) shows the chemical composition of the cones before biosorption. This is qualitatively and quantitatively determined by the EDS analysis and given in Figure 2(c). The EDS spectrum confirmed that the cones are chemically composed of carbon, oxygen, and potassium. After the biosorption, the amount (wt.%) of C, O and K decreased from (52.2, 45.7, and 2.1 (wt.%)) to (50.4, 45.2, and 0 (wt.%)). The heavy metals (Pb^{2+}, Cu^{2+}, Cd^{2+}, Ni^{2+}, and Co^{2+}) were qualitatively determined by EDS analysis and are shown in Figure 2(d). This condition suggested that the biosorption of the metal ions might include an ion-exchange mechanism.

Influence of the concentration on the biosorption efficiency and capacity of the heavy metal ions in the quinary system

The biosorption efficiency and capacity of Pb^{2+}, Cu^{2+}, Cd^{2+}, Ni^{2+}, and Co^{2+} metal ions according to the concentration are given in Figure 3(a). The experimental investigations were conducted using mixed solutions (20–60 mg L^{-1}). The biosorption efficiency decreased with the increase in the concentration. It was considered that the active sites saturated on the biosorbent caused a reduction in the biosorption efficiency. But, the number of metal ions removed

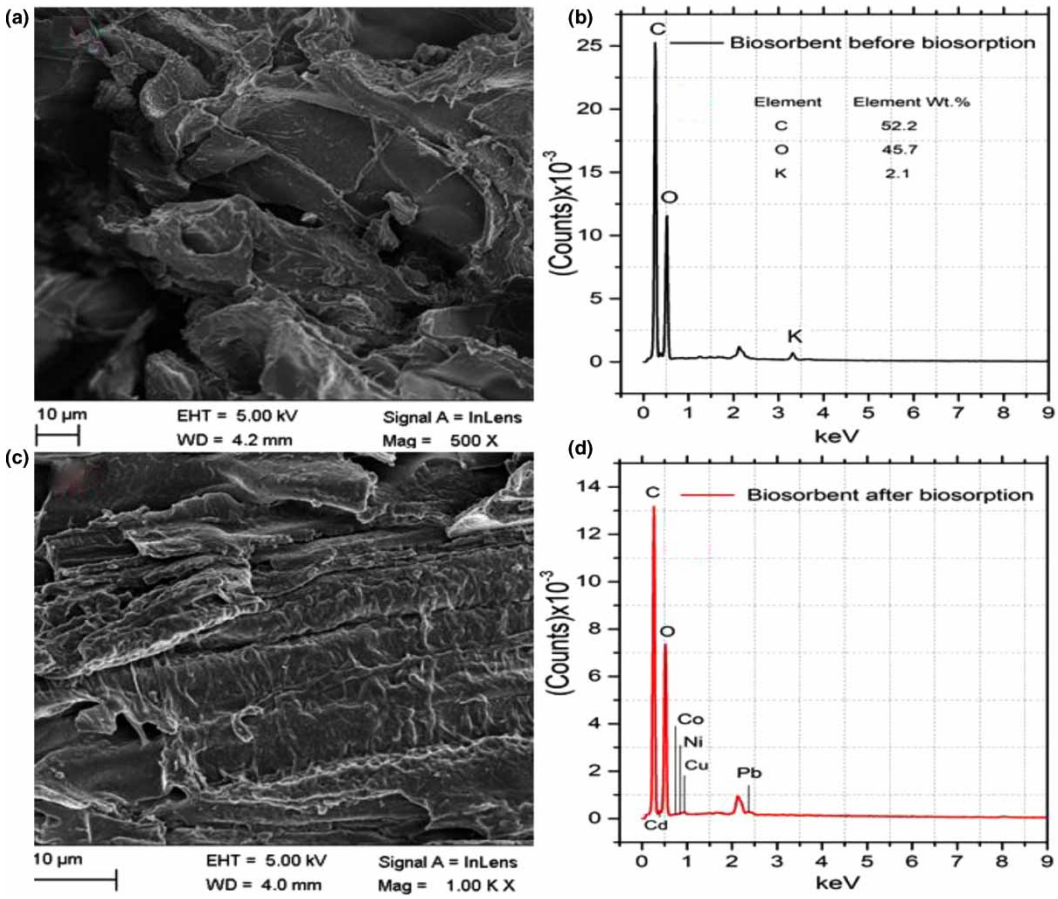

Figure 2 | Characterization of *Abies bornmulleriana* cones: (a, c) SEM image/EDS analysis before the biosorption and (b, d) SEM image/EDS analysis after the biosorption.

per unit mass of the biosorbent increased with the increase in concentration. The ratio of the number of metal ions to the present sites augmented due to the augmentation of the driving force between the metal ions and solid phase (Wang *et al.* 2018). The increase in the biosorption capacity could arise from the increase in electrostatic interaction between the metal ions and sites (Alasheh & Duvnjak 1995). The maximum biosorption efficiency and the minimum biosorption capacity for the metal ions were obtained when the metal ion concentration was 20 mg L^{-1}. After a biosorption contact time of 60 min, the biosorption efficiency and capacity for Pb^{2+}, Cu^{2+}, Cd^{2+}, Ni^{2+}, and Co^{2+} ions were defined as (95, 83.2, 52.3, 40.8 and 33%) and (4.8, 4.15, 2.61, 2.1 and 1.7 mg g^{-1}), respectively. But, the minimum biosorption efficiency and the maximum biosorption capacity for Pb^{2+}, Cu^{2+}, Cd^{2+}, Ni^{2+}, and Co^{2+} ions were obtained as (76.1, 83, 43.6, 25.3, 15.6 and 13.6%) and (11.4, 6.4, 3.8, 2.4 and 2 mg g^{-1}), respectively when the concentration of each ion was 60 mg L^{-1}. The maximum biosorption efficiency and capacity for the metal ions resulted in the magnitude order of $Pb^{2+} > Cu^{2+} > Cd^{2+} > Ni^{2+} > Co^{2+}$.

A possible interpretation for the outcomes is that the ionic radius of Pb^{2+} is bigger than others. The ionic radius of metal ions is in the magnitude order of Pb^{2+} (1.19 Å) > Cd^{2+} (0.95 Å) > Cu^{2+} (0.73 Å) > Ni^{2+} (0.71 Å) > Co^{2+} (0.65 Å). It is thought that the biosorbent sites have a stronger physical affinity for Pb^{2+} ions. Due to Brownian motion, the possibility of collision between Pb^{2+} ions and the biosorbent sites increased with the increase of metal ionic radius. Thus, the biosorption capacity related to Pb^{2+} increased. Similar results published in the literature concerning the biosorption of Pb^{2+}, Cu^{2+}, Cd^{2+}, Ni^{2+}, and Co^{2+} on the different biosorbents show that Pb^{2+} ion has a higher biosorption affinity than the other metal ions in multi-ion systems (Nourbakhsh *et al.* 2002; Hawari & Mulligan 2007; Bayo 2012).

In this study, it was defined that the biosorption efficiency and capacity for Cu^{2+} ion were bigger than those of Cd^{2+} ions. Therefore, the selectivity order did not

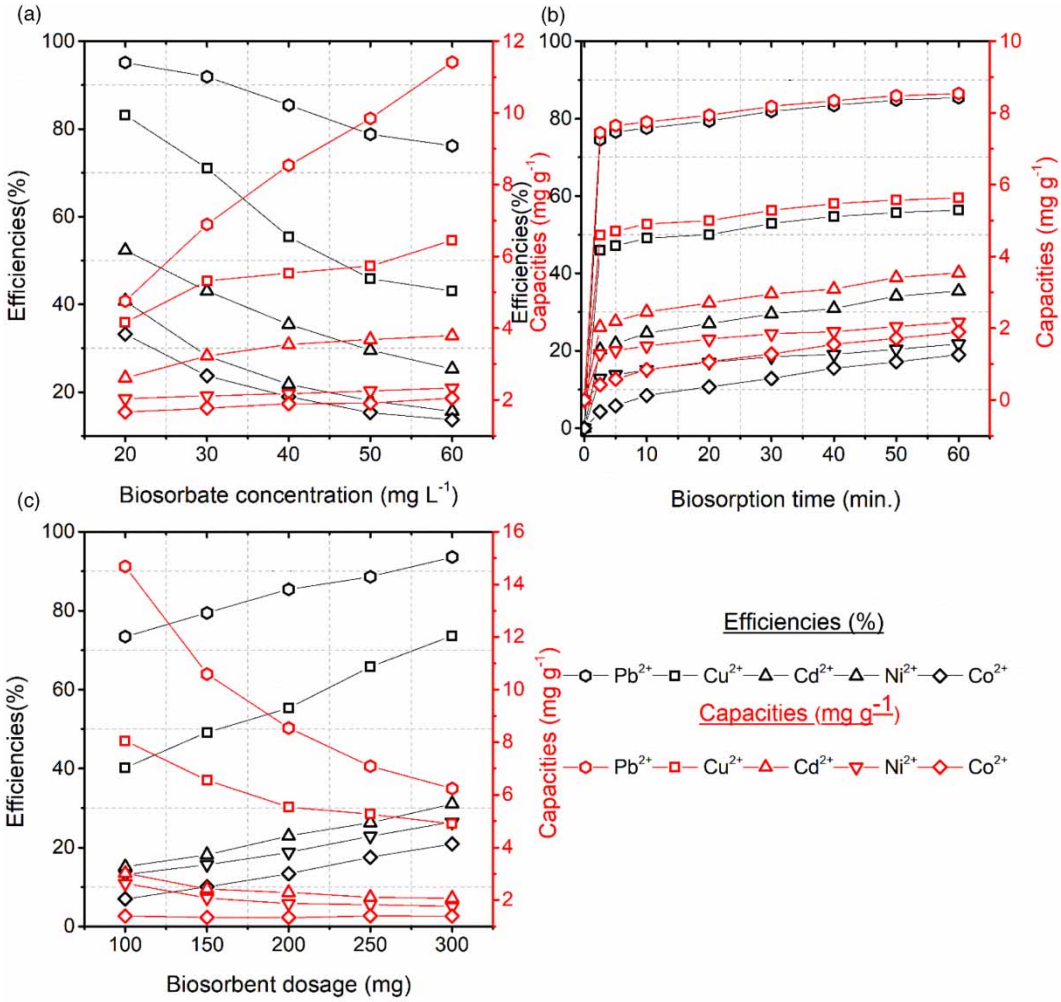

Figure 3 | (a) Influence of the concentration on the biosorption efficiencies and capacities of the heavy metal ions (pH 5, T 20 °C, A.R 250 rpm, P.S 0.125–0.250 mm, B.Q 90 mg, t 60 min and V 50 mL), (b) influence of the contact time on the biosorption efficiencies and capacities of the heavy metal ions (pH 5, T 20 °C, A.R 250 rpm, P.S 0.125–0.250 mm, B.Q 90 mg, and V 50 mL), and (c) influence of the biosorbent quantity on the biosorption efficiencies and capacities of the heavy metal ions (pH 5, T 20 °C, A.R 250 rpm, P.S 0.125–0.250 mm, Con. 40 mg L^{-1}, t 60 min and V 50 mL).

correlate precisely the ionic radius order of the metal ions. The electronegativity (1.95 Pauling scale) of Cu^{2+} ion is higher than the electronegativity (1.69 Pauling scale) of Cd^{2+} ion. But, the hydrated radius (4.19 Å) of Cu^{2+} ion is smaller than the hydrated radius (4.26 Å) of Cd^{2+} ion. It was thought that these two criteria were more effective than the magnitude order of the ionic radius of both metal ions. In the competitive biosorption, the complicated interactions, including ionic radius, hydrated radius, the electron affinity of the ions, and functional properties of the biosorbent, would affect removal of the Cd^{2+} ions, and almost suppressed its biosorption capacity. The metal ions with higher electronegativity are strongly attracted by the biosorbent. Additionally, it is thought that the functional groups (OH, -CONH- and C-O-C) availability on the biosorbent have more affinity to bind Cu^{2+} ions than Cd^{2+} metal ions.

Influence of the contact time on the biosorption efficiency and capacity of the heavy metal ions in the quinary system

A series of contact times from 0 to 60 minutes for the biosorption of Pb^{2+}, Cu^{2+}, Cd^{2+}, Ni^{2+}, and Co^{2+} ions was examined at 40 mg L^{-1} and 20 °C. It is seen from Figure 3(b) that the biosorption efficiency and capacity of metal ions increased very fast within the first 20 minutes due to the sufficient availability of binding sites. However, an increase over 20 minutes describes an inconsiderable improvement in the biosorption performance.

The biosorption approached the equilibrium state within approximately 60 min. The biosorption efficiency and capacity of metal ions at various contact times are shown in Figure 3(b). The biosorption efficiency and capacity of Pb^{2+}, Cu^{2+}, Cd^{2+}, Ni^{2+}, and Co^{2+} ions for a time of 60 minutes were determined as (85.5, 56.4, 35.4, 21.8 and 18.9%) and (8.5, 5.6, 3.5, 2.2 and 1.9 mg g^{-1}), respectively. The variation in the biosorption of the metal ions was interpreted with the variation in the ionic size of the metal ions and the nature of active groups on the biosorbent surface (Okieimen *et al.* 1985). The findings were in good agreement with the first researches, in which biosorption took place between 10 and 20 min. (Bourliva *et al.* 2013). Extra progress in the time did not end in an excessive increase in the biosorption efficiency and capacity.

Influence of the biosorbent quantity on the biosorption efficiency and capacity of the heavy metal ions in the quinary system

The influence of the biosorbent quantity (BQ) on efficiency and capacity was examined at the various quantities ranging from 0.25 to 0.75 g L^{-1}, and the conclusions were given in Figure 3(c). The efficiency of biosorption for Pb^{2+}, Cu^{2+}, Cd^{2+}, Ni^{2+}, and Co^{2+} ions increased with the increase of biosorbent quantity while the biosorbent capacities of these ions decreased. The increase in the efficiency arising from the biosorbent quantity caused a rise in the surface area and binding sites of the biosorbent. Thus, the efficiency of biosorption for the metal ions augmented, respectively. The maximum biosorption efficiency was obtained at the biosorbent amount of 300 mg. Besides, as shown from Figure 3(c), the quantity of metal ions removed per unit biosorbent decreased with the increase of biosorbent quantity. It was thought that the low concentration of metal ions caused the low biosorption capacity, as seen in Figure 3(c). Additionally, the high biosorbent quantity enhanced the possibility of collision between the biosorbent particles. Thus, the aggregation of the biosorbent particles induced a reduction in the biosorbent surface area and an expansion in the diffusional pathway. It was thought that these reasons contributed to a decrease in biosorption capacities (Chen *et al.* 2012). After a time of 60 min, the minimum biosorption efficiency and maximum biosorption capacity for Pb^{2+}, Cu^{2+}, Cd^{2+}, Ni^{2+}, and Co^{2+} metal ions were obtained as (73.4, 40.3, 15.1, 13.1 and 6.8%) and (14.7, 8.1, 3.1, 2.6 and 1.4 mg g^{-1}) respectively. In contrast, the maximum biosorption efficiency and the minimum biosorption capacity for Pb^{2+}, Cu^{2+}, Cd^{2+}, Ni^{2+}, and Co^{+2} metal ions were defined as (93.6, 73.6, 31.1, 26.4 and 20.9%) and (6.2, 4.9, 2.1, 1.7 and 1.4 mg g^{-1}), respectively.

Influence of the particle size on the biosorption efficiency and capacity of the heavy metal ions in the quinary system

The influence of particle size (P.S) on the biosorption efficiency and capacity were studied in the range of 0.125–0.25 to 1–2 mm. The biosorption efficiency and capacity of Pb^{2+}, Cu^{2+}, Cd^{2+}, Ni^{2+}, and Co^{2+} metal ions increased with the decrease of particle size, as given in Figure 4(a). It was thought that this increase was due to the high mass transfer in the particles of small size. The biosorption efficiency and capacity for Pb^{2+}, Cu^{2+}, Cd^{2+}, Ni^{2+}, and Co^{2+} metal ions decreased from (91.8, 64.8, 40.1, 27.1 and 23.1%) and (9.2, 6.5, 4.1, 2.7 and 2.3 mg g^{-1}) to (64.2, 35.7, 19.7,13.1 and 7.9%) and (6.4, 3.6, 1.9, 1.3 and 0.8 mg g^{-1}), respectively when the particle size increased from 0.125–0.250 to 1–2 mm. The BET surface area and pore volume of the biosorbent before and after the biosorption were defined to be (5.05 m^2 g^{-1} and 0.0018 cm^3 g^{-1}) and (0.97 m^2 g^{-1} and 0.00032 cm^3 g^{-1}), respectively. The average pore width of the biosorbent before and after the biosorption was calculated to be 9.34 and 13.04 Å, respectively. The decrease in the surface area and pore volume of the biosorbent and the increase in the particle size after biosorption emphasizes that the metal ions were retained on the biosorbent.

Influence of the pH on the biosorption efficiency and capacity of the heavy metal ions in the quinary system

The removal of Pb^{2+}, Cu^{2+}, Cd^{2+}, Ni^{2+}, and Co^{+2} metal ions were researched at the various pH values ranging from 3 to 5.8, and conclusions are given in Figure 4(b). The experimental studies were not conducted above pH 5.8 to avoid any metal hydroxide precipitation. It is known that metal ions [M(II) = Pb^{2+}, Cu^{2+}, Cd^{2+}, Ni^{2+}, and Co^{2+}] exist in species of M^{2+}, $M(OH)^{+}$and $M(OH)_{2(s)}$ in deionised water. The biosorption efficiency and capacity of the metal ions augmented when pH augmented from 3 to 5.8. In general, the biosorption efficiency and capacity displayed a downward trend with the decrease of pH. The abundance of H^{+} ions in the low pH values surpasses the number of metal ions, and the biosorbent surface is controlled by H^{+} ions

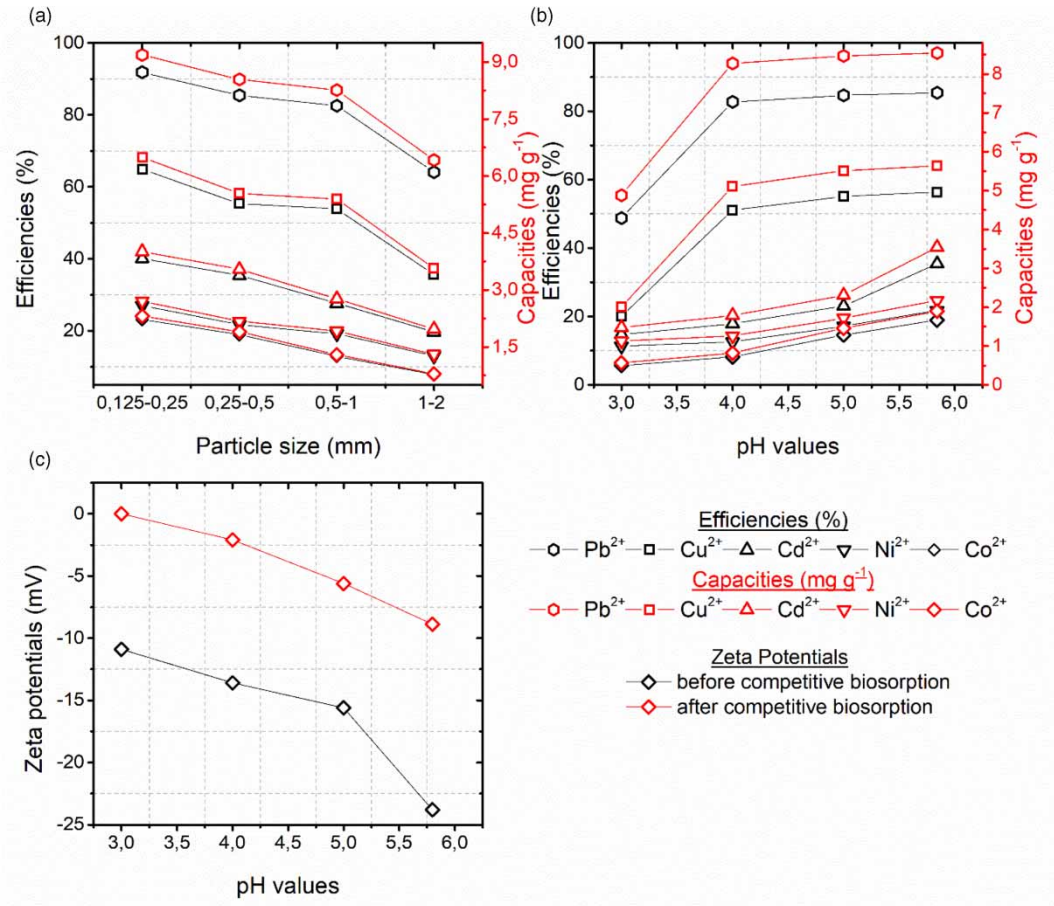

Figure 4 | (a) Influence of the particle size on the biosorption efficiencies and capacities of the heavy metal ions (pH 5, T 20 °C, A.R 250 rpm, B.Q 90 mg, Con. 40 mg L^{-1}, t 60 min and V 50 mL), (b) influence of the pH on the biosorption efficiencies and capacities of the heavy metal ions (T 20 °C, A.R 250 rpm, B.Q 90 mg, P.S 0.125–250 mm, Con. 40 mg L^{-1}, t 60 min and V 50 mL), and (c) the relation between pH and zeta potential values.

(Sen Gupta & Bhattacharyya 2008). More H^+ ions leaving the biosorbent with the increase of pH make the biosorbent sites more suitable for the metal ions, which are bound on the biosorbent surface by the ion exchange mechanism (H^+/Pb^{2+}, H^+/Cu^{2+}, H^+/Cd^{2+}, $H^+/Ni^{2+}$and H^+/Co^{2+}) (Jiang *et al.* 2010; Bourliva *et al.* 2015). Biosorption efficiency and capacity of Pb^{2+}, Cu^{2+}, Cd^{2+}, Ni^{2+}, and Co^{2+} metal ions increased from (48.8, 20.1, 14.7, 11.3 and 5.6%) and (4.8, 2.1, 1.5, 1.2 and 0.6 2.3 mg g^{-1}) to (85.4, 56.4, 35.4, 21.7 and 18.9%) and (8.5, 5.6, 3.5, 2.2 and 1.9 mg g^{-1}), respectively with the increase of pH from 2 to 5.8.

In Figure 4(c), zeta potentials of the biosorbent particles at pH 3, 4, 5, and 5.8 in deionised water were distinct from those of the biosorbent particles containing Pb^{2+}, Cu^{2+}, Cd^{2+}, Ni^{2+}, and Co^{2+} metal ions. The changes in the zeta potential of the charged biosorbents show the uptake of the metal ions from the quinary system. It was thought that Pb^{2+}, Cu^{2+}, Cd^{2+}, Ni^{2+}, and Co^{2+} metal ions attracted by the loads on the biosorbent were adsorbed on the biosorbent surface. Thus, a positive increase in the zeta potentials occurred, as seen in Figure 4(c). The variations in the zeta potentials were evidence of the biosorption of metal ions.

Influence of the temperature on the biosorption efficiency and capacity of the heavy metal ions in the quinary system

Influence of the temperature on the removal of Pb^{2+}, Cu^{2+}, Cd^{2+}, Ni^{2+}, and Co^{2+} metal ions was investigated at temperatures ranging from 20 to 50 °C and are presented in Figure 5(a). The biosorption efficiency and capacity for the metal ions augmented with the augmentation of the temperature. This result is reasonably assigned to the swelling impact in the internal structure of the biosorbent due to the high temperatures. It was thought that a specific increase in the temperature facilitated the penetration of metal ions

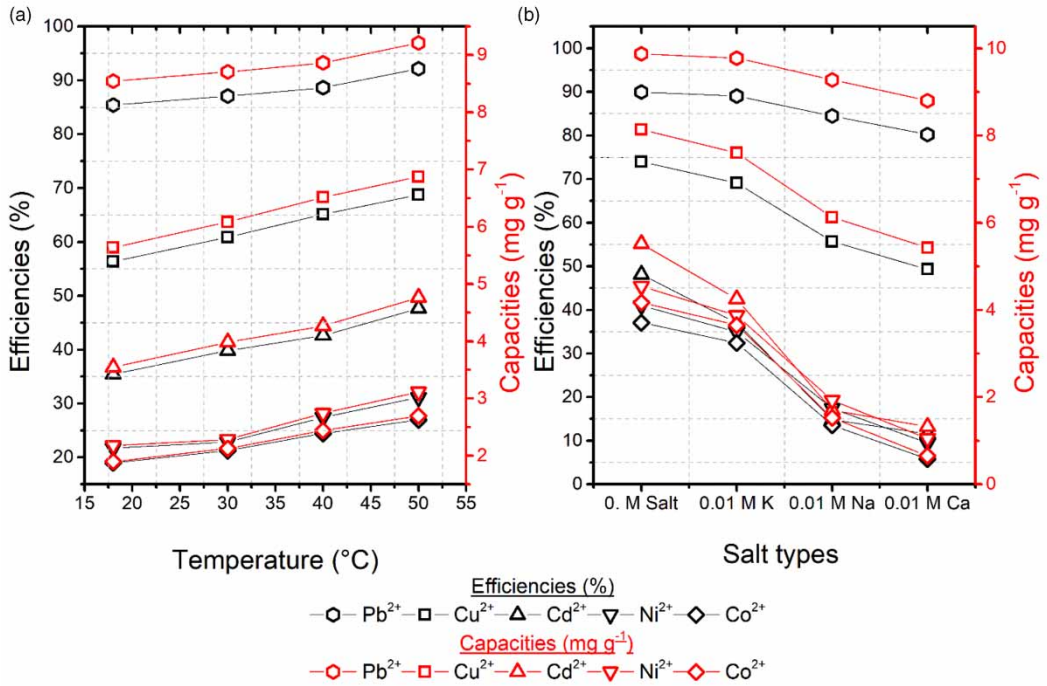

Figure 5 | (a) Influence of the solution temperature on the biosorption efficiencies and capacities of the heavy metal ions (pH 5, A.R 250 rpm, B.Q 90 mg, P.S 0.125–0.250 mm, Con. 40 mg L^{-1}, t 60 min and V 50 mL) and (b) influence of the salt types on the biosorption efficiencies and capacities of the heavy metal ions (pH 5, T 20 °C, A.R 250 rpm, B.Q 90 mg, P.S 0.125–0.250 mm, Con. 40 mg L^{-1} and V 50 mL).

through the biosorbent pores to bind the functional groups on the biosorbent (Zhang *et al.* 2016). The biosorption efficiency and capacity of Pb^{2+}, Cu^{2+}, Cd^{2+}, Ni^{2+}, and Co^{2+} metal ions increased from (85.4, 56.3, 35.4, 21,7 and 18.9%) and (8.5, 5.6, 3.5, 2.2, 1.9 mg g^{-1}) to (92.2, 68.4, 47.6, 31.2 and 26.9%) and (9.2, 6.8, 4.3, 3.1 and 2.7 mg g^{-1}), respectively with the increase of temperature from 20 to 50 °C.

Influence of the salt types on the biosorption efficiency and capacity of the heavy metal ions in the quinary system

The effect of various salts having a concentration of 0.01 M on the biosorption was examined to understand the importance of ionic strength, and findings are presented in Figure 5(b). The decrease of the biosorption capacity for the metal ions displays that biosorption of the metal ions depends on ionic strength. It was believed that the salt addition varied the electrical double layer feature. This process limited the metal ions' transfer from solution to the biosorbent surface (Krishnan & Anirudhan 2002). Moreover, the salt ions compete with Pb^{2+}, Cu^{2+}, Cd^{2+}, Ni^{2+}, and Co^{+2} species for binding to the biosorbent sites. Their binding to the biosorbent sites causes a reduction in Pb^{2+}, Cu^{2+}, Cd^{2+}, Ni^{2+}, and Co^{2+} biosorption. Furthermore, the various types of salt also exhibit various effects on the biosorption of metal ions at equal salt concentration. Ca^{2+} ions have twice the ionic strength compared to Na^{+} and K^{+} ions. Thus, its impact on the electrical double layer in the solution is more effective than Na^{+} and K^{+}. However, the Na^{+} and K^{+} ions, having an equal number of charges, display a similar influence on the electrical double layer. The ionic radius is effective in controlling the competitive biosorption. The average pore width of the biosorbent used in this study was determined to be 9.34 Å, which is bigger than the ionic radius of the salt ions. Na^{+} ions, having higher ionic diameter than K^{+} ions, can more easily compete with the metal ions for the sites present on the biosorbent. As a consequence, the addition of the different types of salts into the solution reduced the biosorption of Pb^{2+}, Cu^{2+}, Cd^{2+}, Ni^{2+}, and Co^{2+} ions in the smallness order of $K^{+} < Na^{+} < Ca^{2+}$ as shown in Figure 5(b). The biosorption efficiency and capacity of Pb^{2+}, Cu^{2+}, Cd^{2+}, Ni^{2+}, and Co^{2+} metal ions in the presence of Ca^{2+}, Na^{+} and K^{+} ions were determined as [(80.2, 49.3, 11.5, 9.5 and 5.8%) and (8.1, 4.9, 1.2, 0.9 and 0.6 mg g^{-1})], [(84.5, 55.6, 17.4, 13.6 and 11.6%) and (8.5, 5.6, 1.7, 1.4 and 1.2 mg g^{-1})] and [(89.2, 69.1, 37.1, 34.9 and

32.4%) and (8.9, 6.9, 3.7, 3.5 and 3.2 mg g^{-1})], respectively when the salt concentration for Ca^{2+}, Na^{+} and K^{+} was 0.01 M.

Equilibrium isotherms

Isotherm models are the equilibrium relations between the concentration of biosorbate on the biosorbent and its concentration in the liquid phase. Isotherm constants ensure the knowledge of the ability of the biosorbent or the quantity needed to uptake a unit mass of heavy metal ions under the experimental conditions. The experimental data were adapted to four different isotherms: Langmuir, Freundlich, Temkin, and Dubinin-Radushkevich.

The Langmuir isotherm (Langmuir 1918) is adequate for monolayer biosorption, which is given by Equation (1).

$$\frac{C_{eq}}{q} = \frac{1}{b_L q_{m,L}} + \frac{C_{eq}}{q_{m,L}} \quad (1)$$

where b_L and $q_{m,L}$ are the Langmuir constant (L mg^{-1}) and the maximum capacity of the biosorbent (mg g^{-1}), respectively (Davis *et al.* 2003). The isotherm models related to the biosorption of Pb^{2+}, Cu^{2+}, Cd^{2+}, Ni^{2+}, and Co^{2+} metal ions are given in Figure 6. D-R model has the highest R^2 value among the four models, as seen in Table 1.

Freundlich isotherm (Freundlich 1906) based on adsorption on a heterogeneous surface having adsorption energy, is

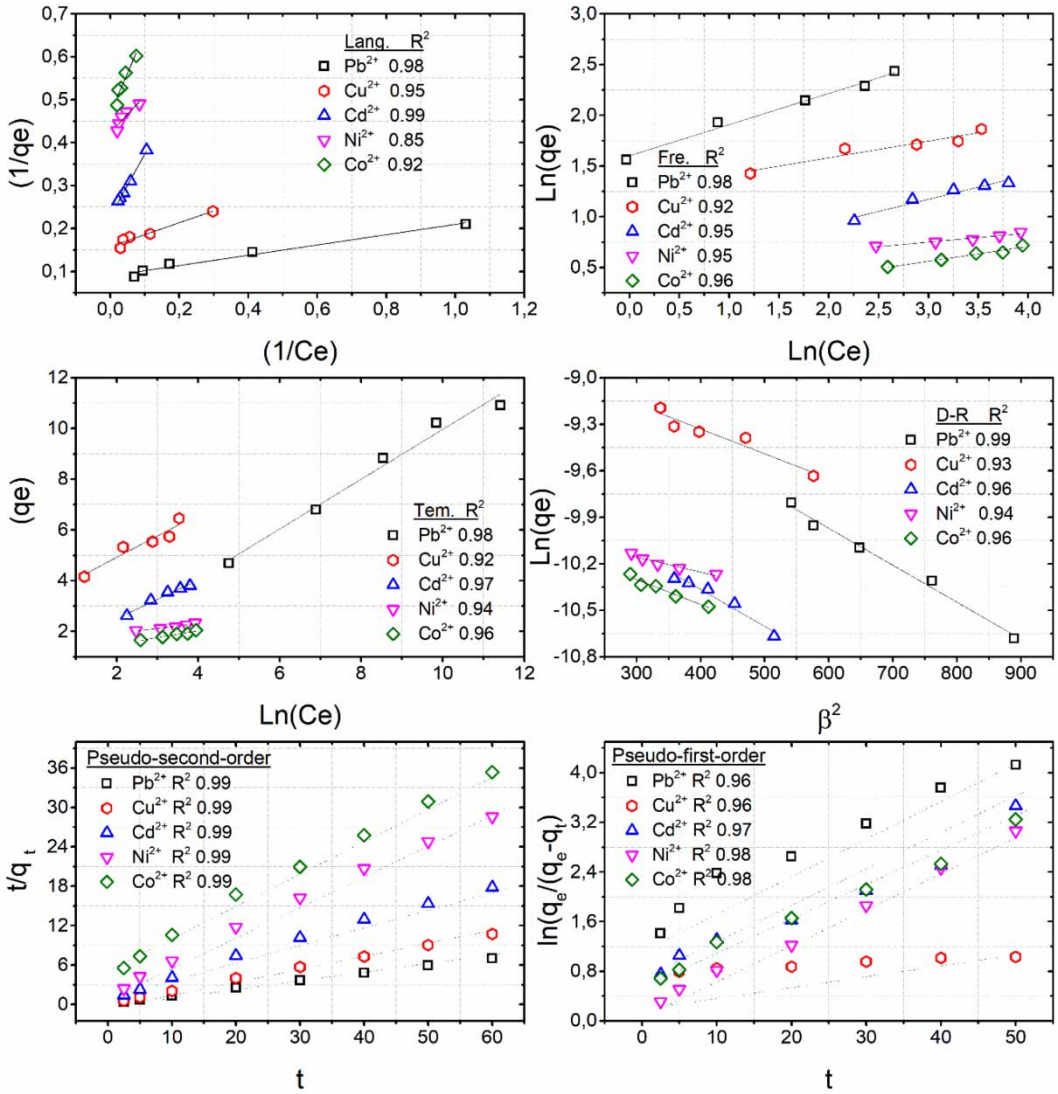

Figure 6 | Isotherm models related to the competitive biosorption of the heavy metal ions and kinetic plots of the heavy metal ions onto *Abies bornmulleriana* cones.

Table 1 | The constants and the correlation coefficients related to Isotherm models

	***Abies bornmulleriana* cone**				
Isotherm models	**Pb^{2+}**	**Cu^{2+}**	**Cd^{2+}**	**Ni^{2+}**	**Co^{2+}**
Langmuir					
$q_{m,L}$ (mg g^{-1})	11.14	6.33	4.37	2.36	2.13
b_L (L mg^{-1})	0.75	056	0.16	0.49	0.25
R^2	0.98	0.95	0.99	0.85	0.92
Freundlich					
K_F	4.96	3.50	1.58	1.62	1.13
n_F	3.25	6.09	4.17	11.12	6.83
R^2	0.98	0.92	0.95	0.95	0.96
Dubinin-Radushkevich					
q_{D-R} (mol g^{-1})	1.9510^{--4}	1.6810^{--4}	8.1910^{--5}	5.210^{--5}	5.4810^{--5}
β_{D-R}	0,0024	0.0016	0.0025	0.001	0.0016
E (kJ mol^{-1})	14.43	17.67	14.14	22.36	17.67
R^2	0.99	0.94	0.97	0.96	0.96
Temkin					
K_{Te} (L g^{-1})	7.75	45.17	3.62	25.54	34.47
b_{Te} (kj $kmol^{-1}$)	2.32	0.85	0.76	0.19	0.26
R^2	0.98	0.92	0.97	0.94	0.96

given by Equation (2).

$$\ln(q_e) = \ln(K_F) + \frac{1}{n_F}\ln C_e \quad (2)$$

where K_F is the Freundlich constant (L g^{-1}), and n_F is the Freundlich exponent. The parameters related to the Freundlich model are shown in Table 1.

The Temkin isotherm is related to the biosorbent-biosorbate synergies. The linear model of the Temkin isotherm (Temkin & Pyzhev 1940) is represented by Equation (3).

$$q_e = \left(\frac{RT}{b_T}\right)\ln A_T + \left(\frac{RT}{b_T}\right)\ln C_e \quad (3)$$

where b_T is a constant linked to the heat of biosorption (J mol^{-1}), A_T is an isotherm constant (L g^{-1}), R the gas constant (8.314 J mol^{-1} K^{-1}) and T the absolute temperature (K). The parameters related to the Temkin isotherm are given in Table 1.

A different famous equation to examine isotherms is proposed by Dubinin (Dubinin & Radushkevich 1947). He stated that the biosorption curve was relevant to the porous structures in the biosorbent. The D-R isotherm is provided by Equation (4).

$$\ln(q_e) = \ln(q_{D-R}) - K\beta^2 \quad (4)$$

$$\beta = RTln\left(1 + \frac{1}{C_e}\right) \quad (5)$$

where q_D (mg g^{-1}) and K (mol^2 kJ^{-2}) are model constants, respectively, β is the Polanyi potential, and E is the mean energy of biosorption determined by Equation (6).

$$E = \frac{1}{\sqrt{2K}} \quad (6)$$

D-R constants and E values are given in Table 1. The size of E is vital for determining the character of biosorption. E values estimated for Pb^{2+}, Cu^{2+}, Cd^{2+}, Ni^{2+}, and Co^{2+} metal ions were 14.43, 15.67, 14.14, 16.36, and 15.47 kJ mol^{-1}, respectively, which are between 8 and 16 kJ mol^{-1}. E values support that the biosorption of Pb^{2+}, Cu^{2+}, Cd^{2+}, Ni^{2+}, and Co^{2+} metal ions occurred by an ion-exchange mechanism. The parameters related to Dubinin-Radushkevich isotherm are given in Table 1. The D-R isotherm for the biosorption was determined as an

adaptable isotherm due to the high correlation coefficients (R^2), as seen in Table 1.

Biosorption kinetics

The kinetic model of the linear pseudo-first-order (Lagergren 1898; Ahsan *et al.* 2020a) was employed to interpret the experimental data and is given by Equation (7).

$$\ln(q_e - q_t) = \ln(q_e) - k_1 t \quad (7)$$

where q_t and q_e are Pb^{2+}, Cu^{2+}, Cd^{2+}, Ni^{2+}, and Co^{2+} amount adsorbed at t time and equilibrium (mg g^{-1}), respectively, and k_1 is the biosorption rate constant (min^{-1}). Figure 6 exhibits a plot of $\ln(q_e - q_t)$ vs. t.

R^2 values related to the pseudo-first-order equation are shown in Figure 6. R^2 values obtained from the pseudo-first-order equation for all the heavy metal ions were low. Thus, the biosorption did not fit to the pseudo-first-order model.

The linear pseudo-second-order equation (Ho & McKay 1999b; Islam *et al.* 2018) is given by Equation (8)

$$\frac{t}{q_t} = \frac{t}{q_e} + \frac{1}{k_2 q_e^2} \quad (8)$$

where k_2 is the rate constant (g mg^{-1} min^{-1}), Figure 6 presents the plot t/qt vs. t.

R^2 values related to the pseudo-second-order equation for all heavy metal ions were approximately 0.99. Thus, the biosorption of Pb^{2+}, Cu^{2+}, Cd^{2+}, Ni^{2+}, and Co^{2+} metal ions was most adequately interpreted by the pseudo-second-order equation, as seen in Figure 6. The linear lines in the plots display an excellent collaboration among the experimental data. R^2 values related to the pseudo-second-order model are exhibited in Figure 6.

The pseudo-first-order model did not provide an excellent fit related to the experimental data. However, the pseudo-second-order model had the most suitable correlation value (R^2 0.99) for all of the metal ions. The R^2 values indicate that the biosorption of Pb^{2+}, Cu^{2+}, Cd^{2+}, Ni^{2+}, and Co^{2+} metal ions follows pseudo-second-order kinetic.

CONCLUSION

The mesoporous volume of the biosorbents decreased at the pore size of 20 nm while the other mesoporous and macroporous volumes of the biosorbents increased after the biosorption. The BET surface area and pore volume of the biosorbents decreased after the biosorption. The average pore width of the biosorbent after the biosorption was calculated as 9 13.04 Å. The changes in wavenumber and band intensity of FTIR spectrums related to the biosorbent after the biosorption point out the functionalities of the biosorbent surface.

The biosorption efficiency was influenced by surface loading regardless of the kind of ions, and the biosorption efficiencies decreased with the increase of metal ion concentration. But, the quantity of metal ions removed per unit mass of the biosorbent increased with the increase of the multi-metal concentration. The biosorption efficiency and capacity of the metal ions increased very fast within the first 20 minutes due to the sufficient availability of binding sites. However, an increase over 20 minutes emphasizes an inconsiderable improvement in the biosorption performance and the approach to the equilibrium state. The biosorption efficiency increased with the increase of biosorbent quantity while the biosorbent capacity decreased. The biosorption efficiency and capacity of the metal ions increased with the decrease of particle size. The biosorption efficiency and capacity of the metal ions augmented with the augmentation of the pH from 3 to 5.8. The changes in the zeta potential of the charged biosorbents exhibit the removal of metal ions. The biosorption efficiency and capacity of the metal ions increased with the increase of temperature. The biosorption capacity decreased with the availability of the salt concentration, which confirmed that the biosorption depended on ionic strength. The biosorption efficiency and capacity for the metal ions followed the magnitude order of $Pb^{2+} > Cu^{2+} > Cd^{2+} > Ni^{2+} > Co^{2+}$.

The D-R isotherm for the biosorption was determined as an adaptable isotherm model due to the high (R^2) values. Isotherm studies suggested that the biosorption of Pb^{2+}, Cu^{2+}, Cd^{2+}, Ni^{2+}, and Co^{2+} metal ions could not involve various isotherm models. For all the ions, the correlation coefficients estimated from the pseudo-second-order equation were approximately 0.99. Thus, the biosorption of Pb^{2+}, Cu^{2+}, Cd^{2+}, Ni^{2+}, and Co^{2+} heavy metal ions is most appropriately represented by this model.

ACKNOWLEDGEMENTS

Author is grateful to the research council of Atatürk University for providing financial support under the project no: FHD/2019/7080. In addition, I would also like to thank

East Anatolia High Technology Application and Research Center (DAYTAM) for their support in the heavy metal analysis.

DATA AVAILABILITY STATEMENT

All relevant data are included in the paper or its Supplementary Information.

REFERENCES

Ahsan, M. A., Deemer, E., Fernandez-Delgado, O., Wang, H., Curry, M. L., El-Gendy, A. A. & Noveron, J. C. 2019 Fe nanoparticles encapsulated in MOF-derived carbon for the reduction of 4-nitrophenol and methyl orange in water. *Catalysis Communications* **130**, 105753.

Ahsan, M. A., Jabbari, V., Imam, M. A., Castro, E., Kim, H., Curry, M. L., Valles-Rosales, D. J. & Noveron, J. C. 2020a Nanoscale nickel metal organic framework decorated over graphene oxide and carbon nanotubes for water remediation. *Science of The Total Environment* **698**, 134214.

Ahsan, M. A., Santiago, A. R. P., Rodriguez, A., Maturano-Rojas, V., Alvarado-Tenorio, B., Bernal, R. & Noveron, J. C. 2020b Biomass-derived ultrathin carbon-shell coated iron nanoparticles as high-performance tri-functional HER, ORR and Fenton-like catalysts. *Journal of Cleaner Production* **275**, 124141.

Ahsan, M. A., Santiago, A. R. P., Sanad, M. F., Weller, J. M., Fernandez-Delgado, O., Barrera, L. A., Maturano-Rojas, V., Alvarado-Tenorio, B., Chan, C. K. & Noveron, J. C. 2020c Tissue paper-derived porous carbon encapsulated transition metal nanoparticles as advanced non-precious catalysts: carbon-shell influence on the electrocatalytic behaviour. *Journal of Colloid and Interface Science* **581**, 905–918.

Alasheh, S. & Duvnjak, Z. 1995 Adsorption of copper and chromium by aspergillus-carbonarius. *Biotechnology Progress* **11** (6), 638–642.

Asadi, F., Shariatmadari, H. & Mirghaffari, N. 2008 Modification of rice hull and sawdust sorptive characteristics for remove heavy metals from synthetic solutions and wastewater. *Journal of Hazardous Materials* **154** (1–3), 451–458.

Bayo, J. 2012 Kinetic studies for Cd(II) biosorption from treated urban effluents by native grapefruit biomass (*Citrus paradisi* L.): the competitive effect of Pb(II), Cu(II) and Ni(II). *Chemical Engineering Journal* **191**, 278–287.

Begum, S. A., Golam Hyder, A. & Vahdat, N. 2016 Adsorption isotherm and kinetic studies of As (V) removal from aqueous solution using cattle bone char. *Journal of Water Supply: Research and Technology – AQUA* **65** (3), 244–252.

Bourliva, A., Michailidis, K., Sikalidis, C., Filippidis, A. & Betsiou, M. 2013 Lead removal from aqueous solutions by natural Greek bentonites. *Clay Minerals* **48** (5), 771–787.

Bourliva, A., Michailidis, K., Sikalidis, C., Filippidis, A. & Betsiou, M. 2015 Adsorption of Cd(II), Cu(II), Ni(II) and Pb(II) onto natural bentonite: study in mono- and multi-metal systems. *Environmental Earth Sciences* **73** (9), 5435–5444.

Chen, Y. G., He, Y., Ye, W. M., Lin, C. H., Zhang, X. F. & Ye, B. 2012 Removal of chromium(III) from aqueous solutions by adsorption on bentonite from Gaomiaozi, China. *Environmental Earth Sciences* **67** (5), 1261–1268.

Davis, T. A., Volesky, B. & Mucci, A. 2003 A review of the biochemistry of heavy metal biosorption by brown algae. *Water Research* **37** (18), 4311–4330.

Dubinin, M. M. & Radushkevich, L. V. 1947 Equation of the characteristic curve of activated charcoal. *Proceedings of the Academy of Sciences of the USSR. Physical Chemistry Section* **55**, 331–333.

Freundlich, H. 1906 Adsorption in solution. *Phys. Chem. Soc.* **40**, 1361–1368.

Han, R. P., Zou, L. N., Zhao, X., Xu, Y. F., Xu, F., Li, Y. L. & Wang, Y. 2009 Characterization and properties of iron oxide-coated zeolite as adsorbent for removal of copper(II) from solution in fixed bed column. *Chemical Engineering Journal* **149** (1–3), 123–131.

Hawari, A. H. & Mulligan, C. N. 2007 Effect of the presence of lead on the biosorption of copper, cadmium and nickel by anaerobic biomass. *Process Biochemistry* **42** (11), 1546–1552.

Ho, Y. S. & McKay, G. 1999a Competitive sorption of copper and nickel ions from aqueous solution using peat. *Adsorption-Journal of the International Adsorption Society* **5** (4), 409–417.

Ho, Y. S. & McKay, G. 1999b Pseudo-second order model for sorption processes. *Process Biochemistry* **34** (5), 451–465.

Homagai, P. L., Ghimire, K. N. & Inoue, K. 2010 Adsorption behavior of heavy metals onto chemically modified sugarcane bagasse. *Bioresource Technology* **101** (6), 2067–2069.

Hossain, M. A., Ngo, H. H., Guo, W. S., Nghiem, L. D., Hai, F. I., Vigneswaran, S. & Nguyen, T. V. 2014 Competitive adsorption of metals on cabbage waste from multi-metal solutions. *Bioresource Technology* **160**, 79–88.

Hyder, A., Begum, S. A. & Egiebor, N. O. 2014 Sorption studies of Cr (VI) from aqueous solution using bio-char as an adsorbent. *Water Science and Technology* **69** (11), 2265–2271.

Islam, M. T., Hernandez, C., Ahsan, M. A., Pardo, A., Wang, H. & Noveron, J. C. 2017 Sulfonated resorcinol-formaldehyde microspheres as high-capacity regenerable adsorbent for the removal of organic dyes from water. *Journal of Environmental Chemical Engineering* **5** (5), 5270–5279.

Islam, M. T., Saenz-Arana, R., Hernandez, C., Guinto, T., Ahsan, M. A., Kim, H., Lin, Y., Alvarado-Tenorio, B. & Noveron, J. C. 2018 Adsorption of methylene blue and tetracycline onto biomass-based material prepared by sulfuric acid reflux. *RSC Advances* **8** (57), 32545–32557.

Islam, M. T., Hyder, A. G., Saenz-Arana, R., Hernandez, C., Guinto, T., Ahsan, M. A., Alvarado-Tenorio, B. & Noveron, J. C. 2019 Removal of methylene blue and tetracycline from water using peanut shell derived adsorbent prepared by

sulfuric acid reflux. *Journal of Environmental Chemical Engineering* **7** (1), 102816.

Jiang, M. Q., Jin, X. Y., Lu, X. Q. & Chen, Z. L. 2010 Adsorption of Pb(II), Cd(II), Ni(II) and Cu(II) onto natural kaolinite clay. *Desalination* **252** (1–3), 33–39.

Krishnan, K. A. & Anirudhan, T. S. 2002 Removal of mercury(II) from aqueous solutions and chlor-alkali industry effluent by steam activated and sulphurised activated carbons prepared from bagasse pith: kinetics and equilibrium studies. *Journal of Hazardous Materials* **92** (2), 161–183.

Kurniawan, T. A., Chan, G. Y. S., Lo, W. H. & Babel, S. 2006 Comparisons of low-cost adsorbents for treating wastewaters laden with heavy metals. *Science of the Total Environment* **366** (2–3), 409–426.

Lagergren, S. 1898 About the theory of so-called adsorption of soluble substances. *Kungliga Svenska Vetenskapsakademiens Handlinger* **24**, 1–39.

Langmuir, I. 1918 The adsorption of gases on plane surfaces of glass, mica and platinum. *Journal of the American Chemical Society* **40**, 1361–1403.

Laus, R. & de Favere, V. T. 2011 Competitive adsorption of Cu(II) and Cd(II) ions by chitosan crosslinked with epichlorohydrin-triphosphate. *Bioresource Technology* **102** (19), 8769–8776.

Liu, C., Ngo, H. H., Guo, W. S. & Tung, K. L. 2012 Optimal conditions for preparation of banana peels, sugarcane bagasse and watermelon rind in removing copper from water. *Bioresource Technology* **119**, 349–354.

Liu, M.-k., Liu, Y.-y., Bao, D.-d., Zhu, G., Yang, G.-h., Geng, J.-f. & Li, H.-t. 2017 Effective removal of tetracycline antibiotics from water using hybrid carbon membranes. *Scientific Reports* **7**, 43717.

Loukidou, M. X., Zouboulis, A. I., Karapantsios, T. D. & Matis, K. A. 2004 Equilibrium and kinetic modeling of chromium(VI) biosorption by *Aeromonas caviae*. *Colloids and Surfaces A-Physicochemical and Engineering Aspects* **242** (1–3), 93–104.

Martin-Lara, M. A., Blazquez, G., Ronda, A., Rodriguez, I. L. & Calero, M. 2012 Multiple biosorption–desorption cycles in a fixed-bed column for Pb(II) removal by acid treated olive stone. *Journal of Industrial and Engineering Chemistry* **18**, 1006–1012.

Munagapati, V. S., Yarramuthi, V., Nadavala, S. K., Alla, S. R. & Abburi, K. 2010 Biosorption of Cu(II), Cd(II) and Pb(II) by *Acacia leucocephala* bark powder: kinetics, equilibrium and thermodynamics. *Chemical Engineering Journal* **157** (2–3), 357–365.

Nourbakhsh, M. N., Kilicarslan, S., Ilhan, S. & Ozdag, H. 2002 Biosorption of Cr^{6+}, Pb^{2+} and Cu^{2+} ions in industrial waste water on Bacillus sp. *Chemical Engineering Journal* **85** (2–3), 351–355.

Oguz, E. & Ersoy, M. 2010 Removal of Cu^{2+} from aqueous solution by adsorption in a fixed bed column and Neural Network Modelling. *Chemical Engineering Journal* **164** (1), 56–62.

Oguz, E. & Ersoy, M. 2014 Biosorption of cobalt(II) with sunflower biomass from aqueous solutions in a fixed bed column and neural networks modelling. *Ecotoxicology and Environmental Safety* **99**, 54–60.

Oguz, E. & Utku, M. 2019 Pore characterization and FTIR spectras of yellow squash particles and adaptive neuro-fuzzy inference system modelling of the breakthrough curves of reactive blue 21 dyestuff in a fixed-bed column. *Environmental Progress & Sustainable Energy* **38**, S110–S1S7.

Okieimen, F. E., Ogbeifeur, D. E., Nwala, G. N. & Kumsah, C. A. 1985 Binding of cadmium, copper and lead ions with modified cellulose materials. *Bulletin of Environmental Contamination and Toxicology* **34**, 866–870.

Pehlivan, E., Altun, T. & Parlayici, S. 2012 Modified barley straw as a potential biosorbent for removal of copper ions from aqueous solution. *Food Chemistry* **135** (4), 2229–2234.

Peng, B., Chen, L., Que, C., Yang, K., Deng, F., Deng, X., Shi, G., Xu, G. & Wu, M. 2016 Adsorption of antibiotics on graphene and biochar in aqueous solutions induced by π-π interactions. *Scientific Reports* **6**, 31920.

Pereira, F. V., Gurgel, L. V. A. & Gil, L. F. 2010 Removal of Zn^{2+} from aqueous single metal solutions and electroplating wastewater with wood sawdust and sugarcane bagasse modified with EDTA dianhydride (EDTAD). *Journal of Hazardous Materials* **176** (1–3), 856–863.

Saeed, A., Iqbal, M. & Akhtar, M. W. 2005 Removal and recovery of lead(II) from single and multimetal (Cd, Cu, Ni, Zn) solutions by crop milling waste (black gram husk). *Journal of Hazardous Materials* **117** (1), 65–73.

Sen Gupta, S. & Bhattacharyya, K. G. 2008 Immobilization of Pb(II), Cd(II) and Ni(II) ions on kaolinite and montmorillonite surfaces from aqueous medium. *Journal of Environmental Management* **87** (1), 46–58.

Temkin, M. I. & Pyzhev, V. 1940 Kinetics of ammonia synthesis on promoted iron catalyst. *Acta Physiochim. URSS* **12**, 327–356.

Torab-Mostaedi, M., Asadollahzadeh, M., Hemmati, A. & Khosravi, A. 2013 Equilibrium, kinetic, and thermodynamic studies for biosorption of cadmium and nickel on grapefruit peel. *Journal of the Taiwan Institute of Chemical Engineers* **44** (2), 295–302.

Volesky, B. 2007 Biosorption and me. *Water Research* **41** (18), 4017–4029.

Vuorinen, H. S., Juuti, P. S. & Katko, T. S. 2007 History of water and health from ancient civilizations to modern times. *Insights Into Water Management: Lessons From Water and Wastewater Technologies in Ancient Civilizations* **7** (1), 49–57.

Wang, R. Z., Huang, D. L., Liu, Y. G., Zhang, C., Lai, C., Zeng, G. M., Cheng, M., Gong, X. M., Wan, J. & Luo, H. 2018 Investigating the adsorption behavior and the relative distribution of Cd^{2+} sorption mechanisms on biochars by different feedstock. *Bioresource Technology* **261**, 265–271.

Zhang, X. T., Hao, Y. N., Wang, X. M., Chen, Z. J. & Li, C. 2016 Competitive adsorption of cadmium(II) and mercury(II) ions from aqueous solutions by activated carbon from *xanthoceras sorbifolia* bunge hull. *Journal of Chemistry* **2016**, 1–10.

First received 5 September 2020; accepted in revised form 2 November 2020. Available online 12 November 2020